Precision measurement of the crossing between the $(J,M)=(0,0)$ and $(1,1)$ sublevels and fine-structure splittings in $3\,^3P$ helium

Dong-Hai Yang, Patrick McNicholl, and Harold Metcalf

Physics Department, State University of New York, Stony Brook, New York 11794

(Received 13 August 1985)

We have measured the position of the Zeeman level crossing between the $(J,M)=(0,0)$ and $(1,1)$ sublevels of the $3\,^3P$ state of helium. The result, 15.756 195(22) MHz (NMR frequency in water), is in good agreement with earlier, less precise measurements. This value, together with our previous measurement of the (2,2)-(0,0) level crossing, is used to calculate the zero-field fine-structure splitting. We find $E_{02}=8772.517(16)$ MHz between the $J=0$ and 2 states, $E_{12}=658.548(69)$ MHz between the $J=1$ and 2 states, and $E_{01}=8113.969(80)$ MHz between the $J=1$ and 0 states.

INTRODUCTION

In a previous paper[1] (referred to hereafter as I), we reported a precision measurement of the magnetic field at the crossing between the $(J,M)=(2,2)$ and $(0,0)$ sublevels in $3\,^3P$ helium. A variation of time-resolved level-crossing techniques (i.e., quantum beats) was employed to obtain the field-crossing value. In the present paper, we report a similar measurement of the crossing field for the (1,1) and (0,0) sublevels. These two independent measurements, along with a theory of the Zeeman effect, allow us to determine the two fine-structure intervals of $3\,^3P$ He.

There is only one previously reported measurement of the field at this crossing[2] which agrees with our result, although it is 14 times less accurate. The lack of precision stems from the inherently larger width of this crossing relative to that in I, as well as its severe susceptibility to pressure broadening, which played an important role in the work of Ref. 2.

EXPERIMENTAL ARRANGEMENT

The experimental method and apparatus have been described in I in great detail; here we shall only briefly outline the experiment and discuss the differences between the present measurements and those reported in I.

The experiments are performed on an atomic beam to eliminate effects from collisions. A tunable pulsed laser (≈ 389 nm, 1.5 GHz width) is used to excite primarily the levels that cross, thereby reducing the background considerably compared with broadband excitation. A second laser pulse [532 nm, Nd:YAG (yttrium aluminum garnet)], delayed from the first by a fixed time, ionizes the $3\,^3P$ He. The quantum beat is revealed as an oscillation of the photoelectron yield as the magnetic field is swept through its crossing value for the relevant levels.[3] As discussed in I, such laser-induced photoionization detection of the quantum beat signal enhances the sensitivity and provides a well-defined geometry for excitation and detection. Furthermore, the use of long delay times [greater than twice the radiative lifetime and limited only by acceptable signal-to-noise ratio (S/N)] narrows the signal and reduces the effects of a large class of systematic errors.[4] These features combine to allow a very large improvement of the measurement of this crossing compared

with that in Ref. 2.

Because the difference between the g factors for the crossing sublevels considered here is smaller than it was in I (smaller crossing angle, as shown in Fig. 9 of I), the field step size was increased from 300 to 400 Hz (NMR frequency). We also used a longer time delay between the two laser pulses. New NMR probes and marginal oscillators were constructed in order to operate at the higher field (≈ 0.37 T) and hence higher NMR frequency (≈ 15 MHz) of the (1,1)-(0,0) crossing. Both the moveable and fixed probes are now spherical (see Fig. 1) so that there is no correction for diamagnetic shielding.[5] Also, the photoionization spectrum is quite different, and is shown in Fig. 2.

In I, the relevant sublevels differed in their magnetic quantum number by 2 ($\Delta M_J=2$) so that linearly polarized σ light could be used to excite a coherent superposition of the (2,2) and (0,0) levels to produce quantum beats in the photoionization signal. For the (1,1)-(0,0) levels, $\Delta M_J=1$ and a combination of σ and π light is required, e.g., linearly polarized at 45° to the field or circularly polarized light propagating perpendicularly to the field. Although calculations show that either of these polarizations will produce a signal, the circularly polarized case pro-
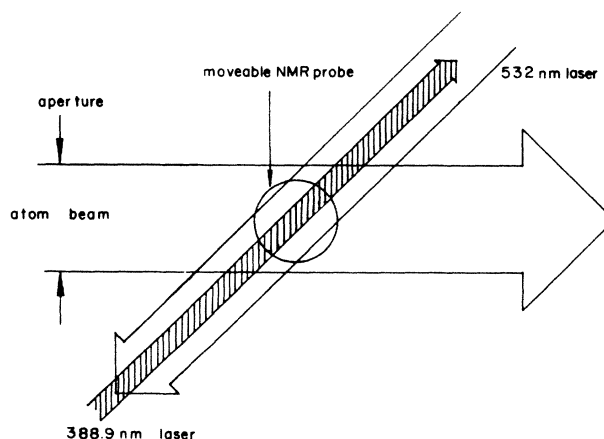

FIG. 1. Experimental geometry showing the overlap of laser and atomic beams in the interaction region with the spherical moveable NMR probe.
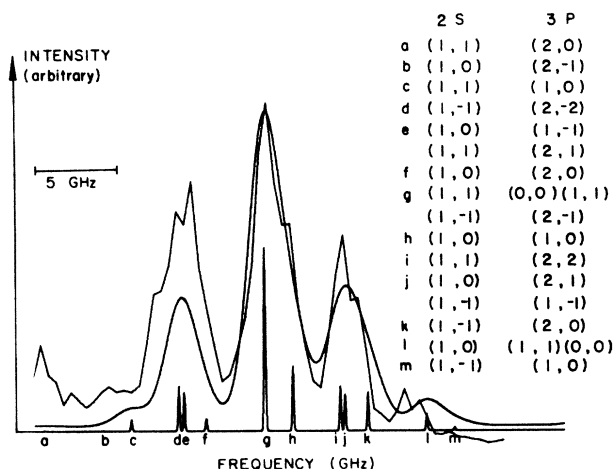
FIG. 2. The photoionization current vs 389 nm laser frequency. Solid line is calculated by convolving shape (labeled) lines with laser width (≈ 1.5 GHz). Jagged line is measured spectrum.

vides a beat modulation depth much larger than the linearly polarized alternative, over four times larger for ionization into D waves. This is a result of the presence of two beat signals from the two continuum M_J states ($M_J = 0$ or 1). In fact, symmetry arguments show that at zero field these beats will have equal amplitude but opposite phase for the linearly polarized case, whereas they will be in phase for the circularly polarized case. Therefore, in the present experiment, quarter-wave plates were used to make the polarizations of the exciting and ionizing lasers circular. (At the crossing field, the signal from linearly polarized light is partially allowed because of mixing of the fine-structure levels produced by the field.)

RESULTS AND ERRORS

The data acquisition process is the same as described in I. We have 80 runs with 220 ns delay between the laser pulses (Table I), mostly consisting of four scans of 15 min each, divided equally between opposite magnetic field directions. Although we see no difference between the two field-reversed populations, having equal numbers tends to cancel errors from certain asymmetries.

For each run, the photoelectron yield versus magnetic field has been fitted with the line shape given in Eq. (1) of I. Figure 3 shows the distribution of fitted center NMR frequencies of Table I in oil (including the field inhomogeneity correction). The standard deviation of this distri-

bution is less than 10 ppm, resulting in a statistical uncertainty of less than 1.1 ppm. From this data we extract the statistical result $f(\text{NMR,oil}) = 15.756\,133(17)$ MHz.

The means of the two populations with opposite fields differ by 0.5(2.1) ppm suggesting an unmeasurably small alignment asymmetry that is mostly canceled by averaging the equal populations using equal weights. Furthermore, a given misalignment produces only half the shift in the present experiment as it did in I. As mentioned in I, the laser beams were aligned to better than 0.002 rad so that the geometric shift will be less than 0.2 ppm. Only a small residue of this shift will survive the equal weighting of reversed-field runs. We estimate it to be less than 0.05 ppm.

The magnet is carefully aligned for optimum homogeneity at this 0.37-T field. The inhomogeneity as shown in Fig. 4 is less than 2 ppm in the interaction region, but our ability to measure it is limited to about 4 ppm. We conservatively estimate that failure to average this over the experimental geometry (Figs. 1 and 3) results in a residual systematic error of less than 0.4 ppm.

We also remeasured the field dependence of the detector gain at this new field of 0.37 T and found it to be even less than it was in I. Also, the systematic error caused by Stark shifts for this crossing has been calculated to be less than 0.06 ppm.

The other possible sources of systematic errors remain the same as they were in I, and all are tabulated as follows: alignment asymmetry, < 0.1 ppm; light shift, 0.1 ppm; inhomogeneity averaging, 0.4 ppm; detector gain, 0.1 ppm; fitting program, 0.1 ppm; Stark effect, < 0.1 ppm. The quadratic sum of these, 0.45 ppm, is combined quadratically with the 1.1-ppm statistical uncertainty resulting in 1.2 ppm. When the measured frequency is converted to NMR frequency in water, the final result $f(\text{water}) = 15.756\,195(22)$ MHz (1.4 ppm) is obtained, where a 0.6 ppm uncertainty has been included for the oil-to-water conversion.[6]

FINE-STRUCTURE SPLITTINGS OF $3\,^3P$ HELIUM

In principle, two different level-crossing measurements in the $3\,^3P$ state of helium and a good Zeeman-effect theory should enable determination of the fine-structure splittings. Lewis, Pichanick, and Hughes have given a Zeeman-effect calculation for $2\,^3P$ helium[7,8] that was applied to the $3\,^3P$ state by Kramer and Pipkin[2] with some parameter adjustments. We follow their procedure below, reproducing some of the equations for completeness. The Zeeman Hamiltonian is $H_{\text{Zeeman}} = H_Z + H_Q$ and its matrix elements are found from

$$\langle JM \mid H_Z \mid J'M \rangle = (-1)^{(1-M)}[6(2J+1)(2J'+1)]^{1/2} \begin{bmatrix} J & 1 & J' \\ -M & 0 & M \end{bmatrix}$$

$$\times \left[\begin{Bmatrix} J & 1 & J' \\ 1 & 1 & 1 \end{Bmatrix} [g'_S + (-1)^{(J+J')}g'_L] + (-1)^J g_x \begin{Bmatrix} 1 & 1 & 2 \\ 1 & 1 & 1 \\ J & J' & 1 \end{Bmatrix} \right] \mu_B H$$

TABLE I. Data of $(J,M) = (1,1)$ and $(0,0)$ measurements.

No.	Center (Hz)	Field correction (Hz)	Delay (ns)	No.	Center (Hz)	Field correction (Hz)	Delay (ns)
1	15 755 943(101)	429	221	41	15 756 037(153)	609	232
2	15 756 224(85)	430	224	42	15 756 382(146)	603	234
3	15 756 158(111)	430	224	43	15 756 116(130)	608	231
4	15 756 237(127)	431	220	44	15 756 224(107)	613	234
5	15 756 314(157)	432	228	45	15 756 227(112)	618	227
6	15 756 161(98)	434	223	46	15 756 471(102)	623	234
7	15 755 903(143)	436	223	47	15 756 139(123)	630	235
8	15 756 126(189)	438	231	48	15 756 158(144)	635	229
9	15 756 303(161)	440	221	49	15 756 232(122)	529	214
10	15 756 235(130)	441	230	50	15 755 976(125)	542	217
11	15 756 099(154)	442	221	51	15 755 918(125)	555	213
12	15 755 870(150)	443	223	52	15 755 980(122)	567	215
13	15 756 097(120)	444	225	53	15 755 879(126)	579	213
14	15 755 862(145)	445	226	54	15 755 816(159)	599	207
15	15 755 940(93)	446	223	55	15 755 870(167)	590	224
16	15 756 114(130)	438	227	56	15 756 185(153)	580	222
17	15 756 220(137)	429	222	57	15 755 987(145)	540	228
18	15 756 092(175)	420	229	58	15 756 056(137)	492	213
19	15 756 153(189)	420	224	59	15 756 204(118)	496	218
20	15 756 169(126)	453	230	60	15 756 223(119)	500	223
21	15 756 215(100)	462	227	61	15 756 255(127)	505	218
22	15 756 126(100)	471	229	62	15 756 173(111)	509	219
23	15 756 249(111)	477	232	63	15 756 245(136)	513	217
24	15 756 103(102)	480	226	64	15 756 408(146)	518	213
25	15 756 217(122)	468	228	65	15 756 171(207)	527	214
26	15 756 138(112)	459	225	66	15 755 682(157)	531	213
27	15 756 112(154)	450	230	67	15 756 057(144)	535	217
28	15 756 198(112)	430	224	68	15 756 101(123)	539	216
29	15 756 011(134)	423	233	69	15 756 362(125)	547	226
30	15 756 265(104)	419	229	70	15 756 100(153)	551	226
31	15 756 130(132)	445	236	71	15 755 889(100)	548	225
32	15 756 323(135)	447	234	72	15 756 049(113)	545	223
33	15 756 072(112)	449	234	73	15 756 254(144)	542	233
34	15 756 038(126)	451	241	74	15 756 289(127)	539	227
35	15 756 110(90)	453	232	75	15 756 198(117)	533	225
36	15 756 303(117)	459	232	76	15 756 094(113)	531	228
37	15 755 715(133)	461	229	77	15 756 125(102)	529	226
38	15 756 182(126)	462	236	78	15 756 365(89)	527	228
39	15 756 079(132)	463	233	79	15 755 839(145)	525	221
40	15 756 229(109)	464	235	80	15 756 085(136)	523	222

and

$$\langle JM \mid H_Q \mid J'M \rangle = (-1)^{(J+J'-M)}[(2J+1)(2J'+1)/12]^{1/2}$$

$$\times \left[\begin{bmatrix} J & 0 & J' \\ -M & 0 & M \end{bmatrix} \begin{Bmatrix} J & 0 & J' \\ 1 & 1 & 1 \end{Bmatrix} (R_{14}+R_{15}) + \left[\frac{2}{5}\right]^{1/2} \begin{bmatrix} J & 2 & J' \\ -M & 0 & M \end{bmatrix} \begin{Bmatrix} J & 2 & J' \\ 1 & 1 & 1 \end{Bmatrix} R_{15} \right] \frac{(\mu_B H)^2}{R_\infty} .$$

Here μ_B is the Bohr magneton, R_∞ is the Rydberg constant for infinite mass, H is the magnetic field, and J and M denote the sublevels of the $3\,^3P$ state (J is not a good quantum number at finite field, but serves as a convenient and well-defined label at the fields of interest here). The parameters R_{14}, R_{15}, g_S', g_L', and g_x for $3\,^3P$ helium are calculated by Kramer and Pipkin[2] from Refs. 7 and 8 as
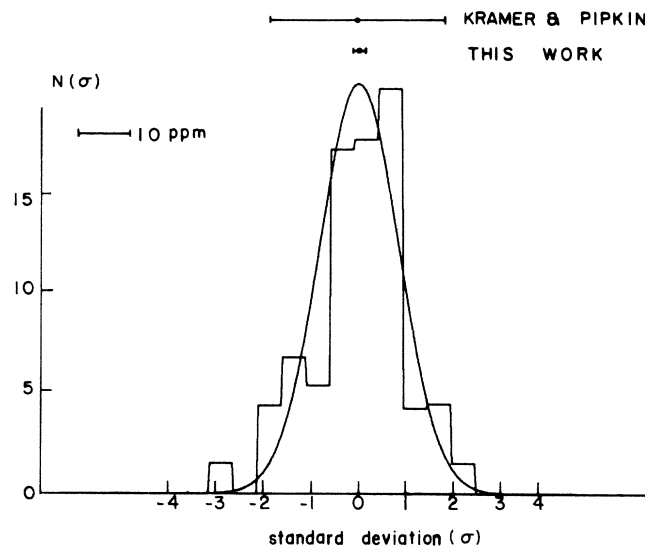
FIG. 3. Histogram of data.

$$g_S' = 2.002\,244\,2(33) \,,$$

$$g_L' = 0.999\,862\,7(28) \,,$$

$$g_x = -0.000\,002\,8(100) \,,$$

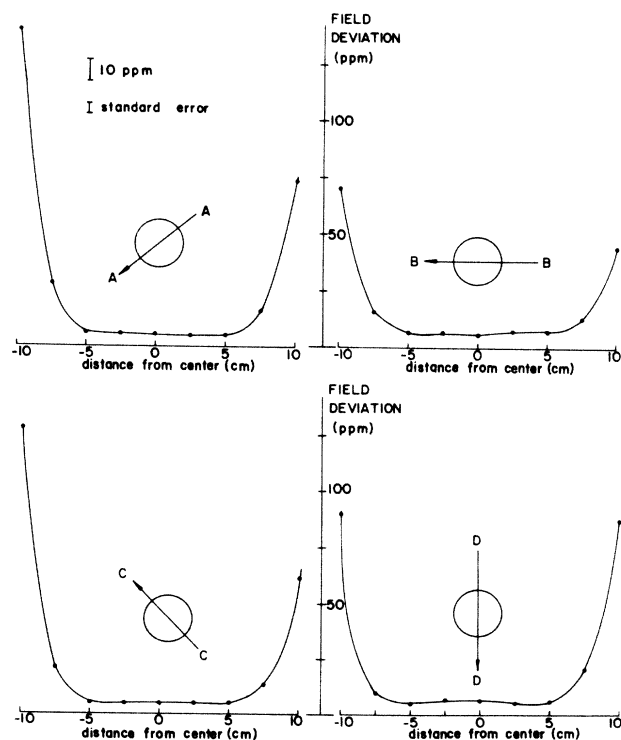$$R_{14} = 0.7520(752) \,,$$

$$R_{15} = 157.69(15.77) \,.$$

FIG. 4. Maps of the magnetic field in four different directions showing very small inhomogeneity (about 1 ppm). Our ability to measure this is about 4 ppm as shown, and our estimate of failure to average this is 10% or 0.4 ppm.

We also use

$$c = 299\,792\,458(12) \text{ m/s,}^9$$

$$R_\infty = 109\,737.3177(83) \text{ cm}^{-1},^9$$

and

$$g_P(\text{water}) = 0.003\,041\,985\,966(34),^{10}$$

whose uncertainties are less than 0.1 ppm and do not contribute to ours.

We can calculate the fine-structure splittings using the formulas above and our measurements directly, propagating the measurement uncertainties appropriately, and obtain the results shown below.[11] However, uncertainties in the Zeeman parameters resulting from approximations in determining the wave functions produce additional uncertainties in the result that, in fact, dominate those from our measurements. The quadratic combination of calculational and measurement uncertainties are also presented below in the last set of parentheses:

$$E_{02} = 8772.517(11) \text{ MHz } (1.3 \text{ ppm}) \ (1.9 \text{ ppm}) \,,$$

$$E_{12} = 658.548(32) \text{ MHz } (48 \text{ ppm}) \ (105 \text{ ppm}) \,,$$

$$E_{01} = 8113.969(26) \text{ MHz } (3.2 \text{ ppm}) \ (9.8 \text{ ppm}) \,.$$

The errors of the parameters in the Zeeman-effect calculation added 1.4, 93, and 9.3 ppm (in quadrature) to E_{02}, E_{12}, and E_{01}, respectively, suggesting that these measurements demand far better calculations than those presently available. In order to compare our work with other measurements, we present a summary in Table II. The present work is a clear improvement over earlier measurements, but presents no serious discrepancies.

TABLE II. Summary of fine-structure measurements.

Interval	Value (MHz)	Reference
E_{20}	8772.330(370)	a
	8772.560(60)	b
	8772.552(40)	c
	8772.517(16)	This work
E_{21}	658(5)	d
	658.550(150)	a
	658.634(271)	c
	658.548(69)	This work
E_{10}	8100(16)	e
	8113.780(220)	a
	8113.750(310)	f
	8113.920(290)	c
	8113.969(80)	This work

[a] Reference 12.   [d] Reference 14.
[b] Reference 13.   [e] Reference 15.
[c] Reference 2.   [f] Reference 16.

CONCLUSIONS

Our new measurement of the level crossing between the (0,0) and the (1,1) sublevels, combined with the measurement reported in I, has been used to determine the fine-structure splittings of the $3\,^3P$ state of neutral helium to unprecedented accuracy. Furthermore, the limitation to the accuracy that can be achieved using these measurements is now dominated by theoretical inaccuracies. Better wave functions and better Zeeman-effect calcula-tions could produce far more accurate fine-structure splitting values. These might be used in conjunction with the results of Frieze et al.[17] as a further test of the helium wave functions and fine-structure calculations.

[1]D. H. Yang and H. Metcalf, Phys. Rev. A 32, 2249 (1985).

[2]P. Kramer and F. Pipkin, Phys. Rev. A 18, 212 (1978).

[3]T. S. Luk, L. DiMauro, and H. Metcalf, Phys. Rev. A 24, 864 (1981).

[4]H. Metcalf and W. Phillips, Appl. Opt. 5, 540 (1980); see also the discussion in Ref. 1.

[5]E. R. Andrew, Nuclear Magnetic Resonance (Cambridge University, Cambridge, England, 1955), p. 78.

[6]B. Taylor, W. Parker, and D. Langenberg, Rev. Mod. Phys. 41, 375 (1969); see also references therein.

[7]M. L. Lewis and V. W. Hughes, Phys. Rev. A 8, 2845 (1973).

[8]S. A. Lewis, F. M. J. Pichanick, and V. W. Hughes, Phys. Rev. A 2, 86 (1970).

[9]E. R. Cohen and B. N. Taylor, J. Phys. Chem. Ref. Data 2, 663 (1973).

[10]W. D. Phillips, W. E. Cooke, and D. Kleppner, Metrologia 13, 179 (1977).

[11]Despite the independence of the two crossing measurements, these calculated values for the fine-structure splittings are not independent. For the sake of statistical completeness and ac-curacy, we note here the correlation coefficients $\rho(E,E')$ for these energies: $\rho(E_{02},E_{12})=-0.587$, $\rho(E_{02},E_{01})=0.713$, $\rho(E_{12},E_{01})=-0.986$.

[12]I. Wieder and W. E. Lamb, Jr., Phys. Rev. 107, 125 (1957).

[13]C. Lhuillier, J. P. Faroux, and N. Billy, J. Phys. (Paris) 37, 335 (1976).

[14]H. G. Berry, T. L. Subtil, and M. Carre, J. Phys. (Paris) 33, 947 (1972).

[15]W. Wittmann, K. Tillmann, H. J. Andra, and P. Dobberstein, Z. Phys. 257, 279 (1972).

[16]R. D. Kaul, J. Opt. Soc. 57, 1156 (1967).

[17]W. Frieze et al., in Precision Measurements and Fundamental Constants II, U.S. Natl. Bur. Stand. Spec. Pub. No. 617, edit-ed by W. Phillips and B. Taylor (U.S. GPO, Washington, D.C., 1984), p. 149.